Seismic characterization of fractured reservoirs: inversion for fracture parameters illustrated using synthetic AVOA data

Mehdi Eftekharifar, University of Houston and Colin M. Sayers, Schlumberger*

Summary

Variations in reflection amplitude as a function of azimuth and incidence angle are sensitive to the presence of natural fractures. Inversion for a second- and a fourth-rank fracture tensor from synthetic *PP*-reflection data with different noise levels from a fractured reservoir with monoclinic symmetry is described. Inversion results are consistent with the corresponding resolution matrices. These can be used for optimum seismic survey design.

Introduction

In the presence of oriented sets of fractures, seismic wave velocities and reflection amplitudes vary with both offset and azimuth. Reflection amplitudes offer advantages over the use of seismic velocities for characterizing fractured reservoirs because they have higher vertical resolution and are more sensitive to the properties of the reservoir. However, the interpretation of variations in reflection amplitude requires a model that allows the measured change in reflection amplitude to be inverted for the characteristics of the fractured reservoir.

In this paper, the variation in the reflection coefficient of seismic *P*-waves as a function of azimuth and offset for two non-orthogonal sets of vertical fractures is used to invert for the components of a second-rank and a fourth-rank fracture compliance tensor. These tensors capture the effect of variable fracture density, compliance, orientation and area on the reflection coefficient. The variation in the trace of the second-rank tensor as a function of position in the reservoir can be used to estimate the variation in fracture density and permeability of the fracture network, and may be used to choose the location of infill wells in the field.

Theory

In the absence of fractures, the elastic stiffness tensor and elastic compliance tensor of the reservoir rock is denoted by C^0_{ijkl} and S^0_{ijkl}, respectively. Sayers and Kachanov (1995) show that the elastic compliance of a fractured reservoir may be written in the form

$$S_{ijkl} = S^0_{ijkl} + \Delta S_{ijkl}, \tag{1}$$

where the excess compliance ΔS_{ijkl} due to the presence of the fractures can be written as

$$\Delta S_{ijkl} = \frac{1}{4}\left(\delta_{ik}\alpha_{jl} + \delta_{il}\alpha_{jk} + \delta_{jk}\alpha_{il} + \delta_{jl}\alpha_{ik}\right) + \beta_{ijkl}. \tag{2}$$

Here, α_{ij} is a second-rank tensor, and β_{ijkl} is a fourth-rank tensor defined by

$$\alpha_{ij} = \frac{1}{V}\sum_r B_T^{(r)} n_i^{(r)} n_j^{(r)} A^{(r)}, \tag{3}$$

$$\beta_{ijkl} = \frac{1}{V}\sum_r \left(B_N^{(r)} - B_T^{(r)}\right) n_i^{(r)} n_j^{(r)} n_k^{(r)} n_l^{(r)} A^{(r)}, \tag{4}$$

where the sum is over all fractures in volume V. $n_i^{(r)}$ is the i^{th} component of the normal to the r^{th} fracture, $A^{(r)}$ is the area of the fracture, and $B_N^{(r)}$ and $B_T^{(r)}$ are the normal and shear compliances of the r^{th} fracture (Sayers and Kachanov, 1995). It is assumed in the following that the fractures are vertical, and that in the absence of fractures the reservoir is either isotropic or transversely isotropic with a vertical axis of rotational symmetry (VTI). Because of space limitations, only equations and inversion results are shown for the case of an isotropic background. If in the absence of fractures, the rock is isotropic or VTI, the elastic symmetry of the fractured rock will be monoclinic for an arbitrary number of vertical fractures with different azimuths. The nonvanishing components of the excess compliance ΔS_{ijkl} due to the presence of the fractures are then (in the conventional two-index notation):

$$\begin{aligned}&\Delta S_{11} = \alpha_{11} + \beta_{1111},\ \Delta S_{22} = \alpha_{22} + \beta_{2222},\ \Delta S_{12} = \Delta S_{21} = \beta_{1122},\\ &\Delta S_{44} = \alpha_{22},\ \Delta S_{55} = \alpha_{11},\ \Delta S_{66} = (\alpha_{11} + \alpha_{22}) + 4\beta_{1122},\\ &\Delta S_{45} = \alpha_{12},\ \Delta S_{16} = \alpha_{12} + 2\beta_{1112}, \text{ and } \Delta S_{26} = \alpha_{12} + 2\beta_{1222}.\end{aligned} \tag{5}$$

The stiffness tensor of the fractured medium can then be determined by inverting the compliance tensor given by equation (1). In this paper the anisotropy and contrast between the overburden and reservoir will be assumed to be small. In this situation, the *P*-wave reflection coefficient for arbitrary elastic symmetry can be written in the form (Pšenčík and Martins, 2001):

$$\begin{aligned}R_{PP}(\theta,\phi) = R_{PP}^{iso}(\theta) + \frac{1}{2}\Delta\varepsilon_z + \frac{1}{2}\Bigg[\left(\Delta\delta_x - 8\frac{\overline{V_s}^2}{\overline{V_p}^2}\Delta\gamma_x\right)\cos^2\phi + \\ \left(\Delta\delta_y - 8\frac{\overline{V_s}^2}{\overline{V_p}^2}\Delta\gamma_y\right)\sin^2\phi + 2\left(\Delta\chi_z - 4\frac{\overline{V_s}^2}{\overline{V_p}^2}\Delta\varepsilon_{45}\right)\cos\phi\sin\phi - \\ \Delta\varepsilon_z\Bigg]\sin^2\theta + \frac{1}{2}\Big[\Delta\varepsilon_x\cos^4\phi + \Delta\varepsilon_y\sin^4\phi + \Delta\delta_z\cos^2\phi\sin^2\phi + \\ 2\left(\Delta\varepsilon_{16}\cos^2\phi + \Delta\varepsilon_{26}\sin^2\phi\right)\cos\phi\sin\phi\Big]\sin^2\theta\tan^2\theta,\end{aligned} \tag{6}$$

where $R_{PP}^{iso}(\theta)$ denotes the weak-contrast reflection coefficient at an interface separating two slightly different isotropic media, and, for vertical fractures, the anisotropy parameters are related to the second-rank and fourth-rank fracture tensors α_{ij} and β_{ijkl} as follows

$$\varepsilon_x = -[(\lambda+2\mu)((\alpha_{11}+\beta_{1111})(\lambda+2\mu)+\beta_{1122}\lambda)+ \lambda(\lambda(\alpha_{22}+\beta_{2222})+\beta_{1122}(\lambda+2\mu))]/2(\lambda+2\mu)$$

$$\varepsilon_y = -[\lambda(\lambda(\alpha_{11}+\beta_{1111})+\beta_{1122}(\lambda+2\mu))+(\lambda+2\mu)((\alpha_{22}+\beta_{2222}) (\lambda+2\mu)+\beta_{1122}\lambda)]/2(\lambda+2\mu)$$

$$\varepsilon_z = -\frac{\lambda^2(\alpha_{11}+\alpha_{22}+\beta_{1111}+2\beta_{1122}+\beta_{2222})}{2(\lambda+2\mu)}$$

$$\varepsilon_{16} = -\frac{2\mu(\alpha_{12}(\lambda+\mu)+\beta_{1112}(\lambda+2\mu)+\beta_{1222}\lambda)}{\lambda+2\mu}$$

$$\varepsilon_{26} = -\frac{2\mu(\alpha_{12}(\lambda+\mu)+\beta_{1222}(\lambda+2\mu)+\beta_{1112}\lambda)}{\lambda+2\mu}$$

$$\varepsilon_{45} = -\mu\alpha_{12} \qquad (7)$$

$$\delta_x = -[\lambda(\alpha_{22}\lambda+\beta_{1111}(\lambda+2\mu)+2\beta_{1122}\lambda+\beta_{2222}\lambda+ 2\beta_{1122}\mu)+\alpha_{11}(\lambda^2+2\lambda\mu+2\mu^2)]/(\lambda+2\mu)$$

$$\delta_y = -[\alpha_{22}(\lambda^2+2\lambda\mu+2\mu^2)+\alpha_{11}\lambda^2+\lambda(2\beta_{1122}(\lambda+\mu) \beta_{2222}(\lambda+2\mu)+\beta_{1111}\lambda)]/(\lambda+2\mu)$$

$$\delta_z = -[\lambda((\alpha_{11}+\beta_{1111})(\lambda+2\mu)+\beta_{1122}\lambda)+(\lambda+2\mu) (\lambda(\alpha_{22}+\beta_{2222})+\beta_{1122}(\lambda+2\mu))-2(\mu- \mu^2(\alpha_{11}+\alpha_{22}+4\beta_{1122}))+2\mu]/(\lambda+2\mu)$$

$$\gamma_x - \frac{\alpha_{11}\mu}{2}, \quad \gamma_y - \frac{\alpha_{22}\mu}{2}, \quad \chi_z = -\frac{2\mu(\alpha_{12}(\lambda+\mu)+(\beta_{1112}+\beta_{1222})\lambda)}{\lambda+2\mu}$$

Here, λ and μ are the second-order elastic constants of the reservoir rock in the absence of fractures. Substitution of equations (7) into equation (6) allows the sensitivities F_{ij} and F_{ijkl} of $R_{PP}(\theta,\varphi)$ to α_{ij} and β_{ijkl} to be determined, where the sensitivity to a parameter is defined to be the angle-dependent coefficient of the parameter in equation (6) as follows (Sayers, 2009):

$$R_{PP}(\theta,\phi) = R_{PP}^{iso}(\theta) + F_{11}(\theta,\phi)\alpha_{11} + F_{12}(\theta,\phi)\alpha_{12} + F_{22}(\theta,\phi)\alpha_{22} + F_{1111}(\theta,\phi)\beta_{1111} + F_{1112}(\theta,\phi)\beta_{1112} + F_{1122}(\theta,\phi)\beta_{1122} + F_{1222}(\theta,\phi)\beta_{1222} + F_{2222}(\theta,\phi)\beta_{2222} \qquad (8)$$

The example considered in this paper consists of fractures added to the type I gas sand of Kim et al. (1993), with *P*-wave velocity of 4.2 km/s, *S*-wave velocity of 2.7 km/s and density 2.49 g/cc in the absence of fractures. The overburden is assumed to be isotropic with *P*-wave velocity of 3.78 km/s, *S*-wave velocity of 2.43 km/s and density of 2.36 g/cc (see Table 1).

Table 1. Parameters for the example shown in this paper.

	v_P [km/s]	v_S [km/s]	ρ [g/cc]
Overburden	3.78	2.43	2.36
Reservoir	4.20	2.70	2.49

Inversion

In this section we examine the extent to which the second- and fourth-rank fracture tensors α_{ij} and β_{ijkl} can be obtained by inversion of AVOA data using synthetic data. Noisy synthetic *PP*-reflection data, calculated using the elastic parameters listed in Table 1, and assuming two sets of vertical fractures embedded either in an isotropic or VTI background, are used for the inversion. In the forward modeling for the example below, the fracture azimuths are taken to be -30 and 50 degrees with respect to the x_1 direction. Fracture sets have different densities with 70% of the contribution to the trace of α_{ij} coming from one set and 30% from the other set. Fracture compliances were chosen to give an overall 10% shear wave splitting if all fractures were parallel. Examples shown in this paper are for the case of an isotropic background, which is assumed to be known (e.g. from sonic and density logs) and constant. The effect of an unknown and variable background medium will be discussed elsewhere. Figure 1 shows two of the acquisition geometry examples considered in this study:

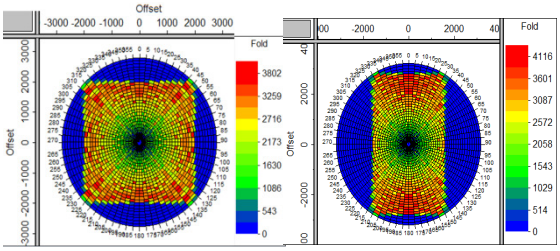

Figure 1: Wide and narrow azimuth data obtained using different acquisition parameters, with the long axis aligned along x_1.

Typical orthogonal seismic survey designs with different patch geometries (different numbers of live receiver lines), which lead to different azimuth/offset content in acquired seismic data, will be compared in the presentation. For the analysis, we chose receiver and shot line intervals of 200m and receiver and shot station intervals of 50m (bin size of 25 m). The depth of the reservoir was assumed to be 2500 m. Different patch aspect ratios (different live receiver lines) were selected to obtain seismic data with different azimuth/offset content. Four cases were considered for inversion and resolution matrix analysis with a) wide azimuth (0-86 degrees) and long offset (0-35 degrees), b)

narrow azimuth (0-45 degrees) and long offset, c) wide azimuth and short offset (0-20 degrees), d) very narrow azimuth (0-30 degrees) and long offset. Noisy reflection coefficient data (Figure 2) obtained using equation (6), were used to invert for the second- and fourth-rank fracture tensors. In Figure 2, the first row shows the reflection coefficient for wide azimuth/long offset, the second row show the narrow offset/long offset case, the third row shows wide azimuth/short offset, and the last row shows the reflection coefficient for the very narrow azimuth/long offset case. In each case, the first column is the total reflection coefficient from the top of fractured layer, the second column is the noisy total reflection coefficient, the third column is the reflection coefficient due only to the fractures, and the last column is the noisy reflection coefficient due to fractures. For inversion, the noisy reflection coefficient due to fractures (last column) is used in each case, and B_N/B_T was taken to be equal to 0.3 for all fractures. Data were sampled at steps of 5 degree in azimuth and 2 degrees (~100 m) in offset, and is assumed to be representative of data obtained by stacking to give an increase in fold and signal to noise ratio (SNR).

The forward problem has the simple form $\boldsymbol{R=Fw}$ where $\boldsymbol{R}$ is a vector of length N containing all measured reflection coefficients, $\boldsymbol{F}$ is an $N \times M$ sensitivity matrix and $\boldsymbol{w}$ is the vector of length M that represents the unknown parameters (components of the second- and fourth-rank fracture tensors). Inversion can be performed using either simple matrix operations, where the solution can be obtained from:

$$\boldsymbol{w} = (\boldsymbol{F}^T\boldsymbol{F})^{-1}\boldsymbol{F}^T\boldsymbol{R} \tag{9}$$

or, more conveniently, using the conjugate gradient method where the problem can be cast in the following form:

$$\boldsymbol{Aw=B} \tag{10}$$

where $\boldsymbol{Aw=FF^Tw}$ and $\boldsymbol{B=FR^T}$.

This can be solved in an iterative manner as follows (Koehler and Taner, 1985):

$$\begin{aligned} &G^0 = P^0 = B - Aw^0 \\ &d^k = \frac{G^k (G^k)^T}{P^k (AP^k)^T},\ w^{(k+1)} = w^k + d^k P^k \\ &G^{(k+1)} = G^k - d^k AP^k,\ g^{(k+1)} = \frac{G^{(k+1)} (G^{(k+1)})^T}{G^k (G^k)^T} \\ &P^{(k+1)} = G^{(k+1)} + g^{(k+1)} P^k \end{aligned} \tag{11}$$

where k is the number of iterations.

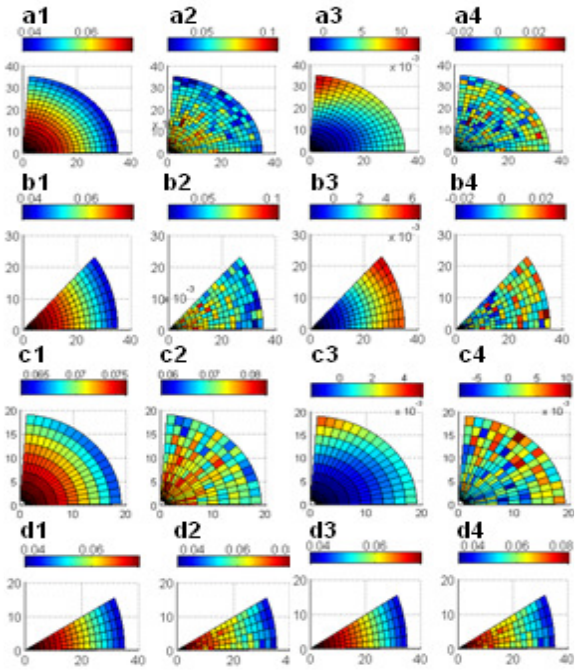

Figure 2: Reflection coefficients for a) wide azimuth/long offset, b) narrow azimuth/long offset, c) wide azimuth/short offset and d) very narrow azimuth/long offset. The long axis is aligned along x_1.

An approximate solution $\boldsymbol{w}^{(k+1)}$ can be found after a sufficient number of iterations. Use of the conjugate gradient method becomes especially important in the case of narrow azimuth or short offset data. Inversion should be preceded by a resolution matrix analysis (see Menke, 1989 and Eftekharifar and Sayers, to be published) to determine the confidence in the inversion for the fracture tensor components. Resolution matrix analysis is controlled by seismic data acquisition geometry and should be used to determine an optimum seismic survey design. Figure 3 a, b, c and d show the resolution matrices for the cases mentioned before. The diagonal elements of the matrices represent the resolution of the α_{ij} and β_{ijkl}. Hot colors for diagonal elements imply better resolution than cooler colors.

Results

Inversion results for the four cases discussed above are shown in figure 4. The right figures in each case are inversion results using reflectivity data with SNR=50 and the left figures are with SNR=40. The vertical axes show the components of the fracture tensors computed by forward modeling and the horizontal axis shows the values obtained from inversion.

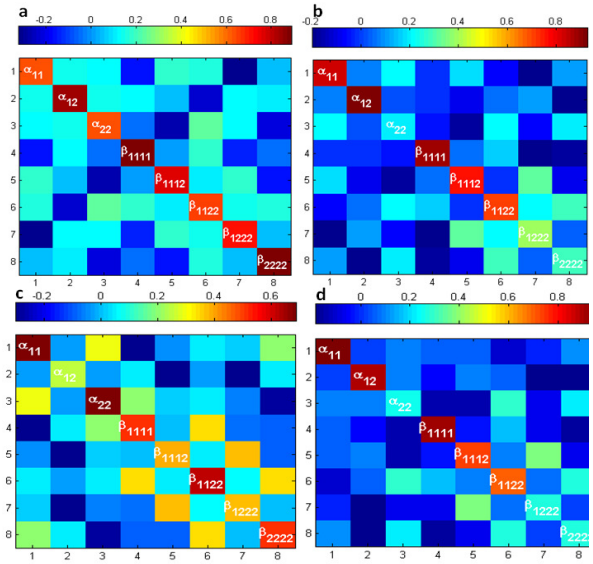

Figure 3: Resolution matrices for a) wide azimuth/long offset, b) narrow azimuth/long offset, c) wide azimuth/short offset and d) very narrow azimuth/long offset.

The components of the second- and fourth-rank fracture tensors are made dimensionless by multiplying by the shear modulus of the background medium. The inversion results are consistent with the computed resolution matrices.

Conclusion

Synthetic AVOA data, with different noise levels, were used to invert for the components of the second- and fourth-rank fracture tensors in a fractured reservoir with monoclinic symmetry. Inversion results are consistent with the corresponding resolution matrices. These can be used for optimum seismic survey design for fracture characterization tasks.

Acknowledgements

The first author thanks De-hua Han for suggesting the area of research, for providing useful background information and financial support via the Fluid and DHI consortium, and for many useful comments and suggestions. We thank Leon Thomsen for helpful comments and discussion.

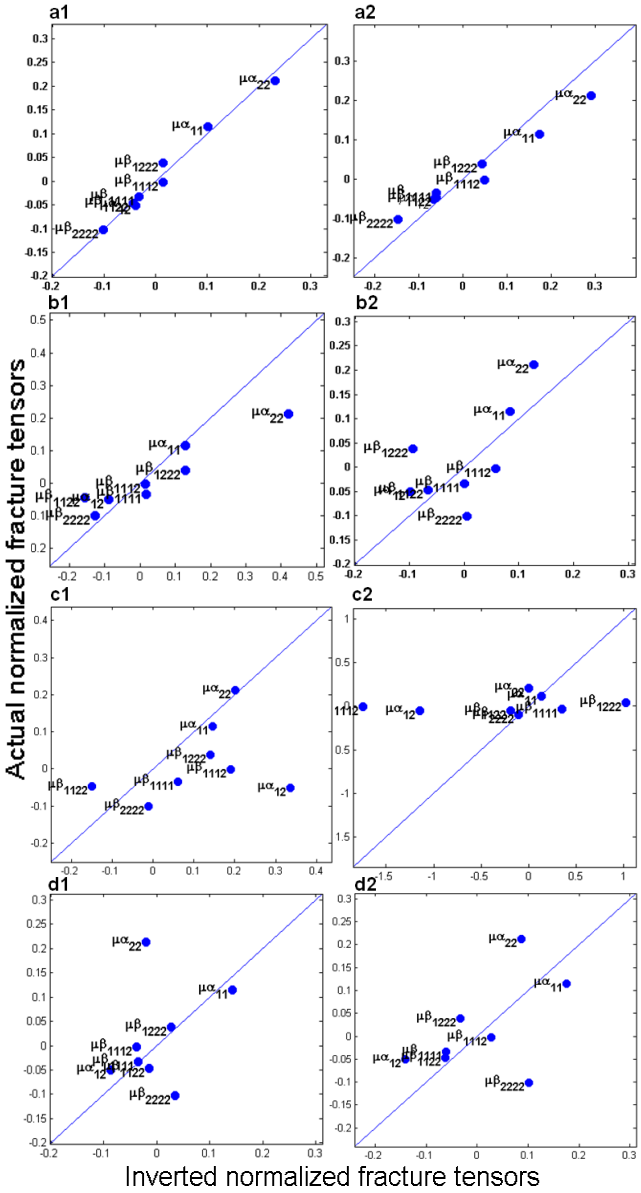

Figure 4: Inversion results for α_{ij} and β_{ijkl} using synthetic reflectivity data. Left column: SNR 50, right column: SNR=40. a) wide azimuth long offset (a1: correlation coefficient=98%. a2: correlation coefficient=94%). b) Narrow azimuth and long offset (b1: correlation coefficient=94%. b2: correlation coefficient=66%). c) wide azimuth and short offset (c1: correlation coefficient =36%. c2: correlation coefficient=24%). d) very narrow azimuth and long offset (d1: correlation coefficient =32%. d2: correlation coefficient=49%).

EDITED REFERENCES

Note: This reference list is a copy-edited version of the reference list submitted by the author. Reference lists for the 2011 SEG Technical Program Expanded Abstracts have been copy edited so that references provided with the online metadata for each paper will achieve a high degree of linking to cited sources that appear on the Web.

REFERENCES

Kim, K. Y., K. H. Wrolstad, and F. Aminzadeh, 1993, Effects of transverse isotropy on *P*-wave AVO for gas sands: Geophysics, **58**, 883–888, doi:10.1190/1.1443472.

Koehler, F., and M. Turhan Taner, 1985, The use of the conjugate-gradient algorithm in the computation of predictive deconvolution operators: Geophysics, **50**, 2752–2758, doi:10.1190/1.1441895.

Menke, W., 1989, Geophysical data analysis: discrete inverse theory: Academic Press.

Pšenčík, I., and J. L. Martins, 2001, Properties of weak contrast PP reflection/transmission coefficients for weakly anisotropic elastic media: Studia Geophysica et Geodaetica, **45**, 176–199, doi:10.1023/A:1021868328668.

Sayers, C. M., 2009, Seismic characterization of reservoirs containing multiple fracture sets: Geophysical Prospecting, **57**, 187–192, doi:10.1111/j.1365-2478.2008.00766.x.

Sayers, C. M., and M. Kachanov, 1995, Microcrack-induced elastic wave anisotropy of brittle rocks: Journal of Geophysical Research., **100**, 4149–4156, doi:10.1029/94JB03134.